Article Name with DOI link to post-print published Version complete citation:

- Gargoum, Suliman A. and Tawfeek, Mostafa H. and El-Basyouny, Karim and Koch, James C. Available sight distance on existing highways: Meeting stopping sight distance requirements of an aging population. Accident Analysis & Prevention. 112(3): 56-68. http://dx.doi.org/10.1016/j.aap.2018.01.001

Article Post-print starts on the next page →

Accident Analysis and Prevention 112 (2018) 56–68

Contents lists available at ScienceDirect

Accident Analysis and Prevention

journal homepage: www.elsevier.com/locate/aap

Available sight distance on existing highways: Meeting stopping sight distance requirements of an aging population

Suliman A. Gargoum*, Mostafa H. Tawfeek, Karim El-Basyouny, James C. Koch

Department of Civil and Environmental Engineering, University of Alberta, Edmonton, AB, T6G 1H9 Canada

ARTICLE INFO

Keywords:
Available sight distance
Road user ability
Human factors
Stopping sight distance limitations
Remote sensing
LiDAR
Aging population safety

ABSTRACT

An important element of highway design is ensuring that the available sight distance (ASD) on a highway meets driver needs. For instance, if the ASD at any point on a highway is less than the distance required to come to a complete stop after seeing a hazard (i.e. Stopping Sight Distance (SSD)), the driver will not be able to stop in time to avoid a collision. SSD is function of a number of variables which vary depending on the driver, the vehicle driven and surface conditions; examples of such variables include a driver's perception reaction time or PRT (i.e. the time required by the driver to perceive and react to a hazard) and the deceleration rate of the vehicle. Most design guides recommend deterministic values for PRT and deceleration rates. Although these values may serve the needs of the average driver, they may not satisfy the needs of drivers with limited abilities. In other words, even if the ASD exceeds required SSD defined in the design guide, it might not always satisfy the needs of all drivers. While it is impossible to design roads that satisfy the needs of all drivers, the fact that most developed countries suffer from an aging population, means that the number of old drivers on our roads is expected to increase. Since a large proportion of old drivers often have limited abilities, it is expected that the general population of drivers with limited abilities on our roads will increase with time. Accordingly, more efforts are required to ensure that existing road infrastructure is prepared to handle such a change. This paper aims to explore the extent to which ASD on highways satisfies the needs of drivers with limited abilities. The paper first develops MATLAB and Python codes to automatically estimate the ASD on highway point cloud data collected using Light Detection and Ranging (LiDAR) remote sensing technology. The developed algorithms are then used to estimate ASD on seven different crash prone segments in the Province of Alberta, Canada and the ASD is compared to the required SSD on each highway. Three different levels of SSD are defined (SSD for drivers with limited ability, AASHTOs SSD requirements and SSD for drivers with high skill). The results show that, when compared to SSD requirements which integrate limitations in cognitive abilities, a substantial portion of the analyzed segments do not meet the requirements (up to 20%). Similarly, when compared to AASHTO's SSD requirements, up to 6% of the analyzed segments do not meet the requirements. In an attempt to explore the effects of such design limitations on safety, the paper also explores crash rates in noncompliant regions (i.e. regions that do not provide sufficient SSD) and compares them to crash rates in compliant regions. On average, it was found that noncompliant regions experience crash rates that are 2.15 and 1.25 times higher than compliant regions for AASHTO's SSD requirements and those integrating driver limitations, respectively. Furthermore, the study found that a significantly higher proportion of drivers involved in collisions in the noncompliant regions were old drivers.

1. Introduction

Minimum Stopping Sight Distance (SSD) is the distance required by a driver to come to a complete stop when a hazard or obstruction presents itself on a roadway. In order to ensure safe and efficient operation of a roadway, design guidelines require that available sight distance (ASD) exceeds the minimum SSD at all points along a roadway. Minimum SSD requirements are calculated using equations derived in design guidelines and are typically a function of speed, the road's grade, the driver's perception reaction time (i.e. the time required for the driver to perceive and respond to the hazard that creates the stopping requirement), and the vehicle's deceleration rate.

Variables like perception reaction time (PRT) and deceleration rate vary depending on driver capabilities, vehicular performance and the situation on hand, however, most highway design guides use deterministic values for those variables. For instance, AASHTO's highway

* Corresponding author.
E-mail addresses: gargoum@ualberta.ca (S.A. Gargoum), mostafa.h.tawfeek@ualberta.ca (M.H. Tawfeek), basyouny@ualberta.ca (K. El-Basyouny), jckoch@ualberta.ca (J.C. Koch).

https://doi.org/10.1016/j.aap.2018.01.001
Received 2 June 2017; Received in revised form 10 December 2017; Accepted 3 January 2018
Available online 06 January 2018

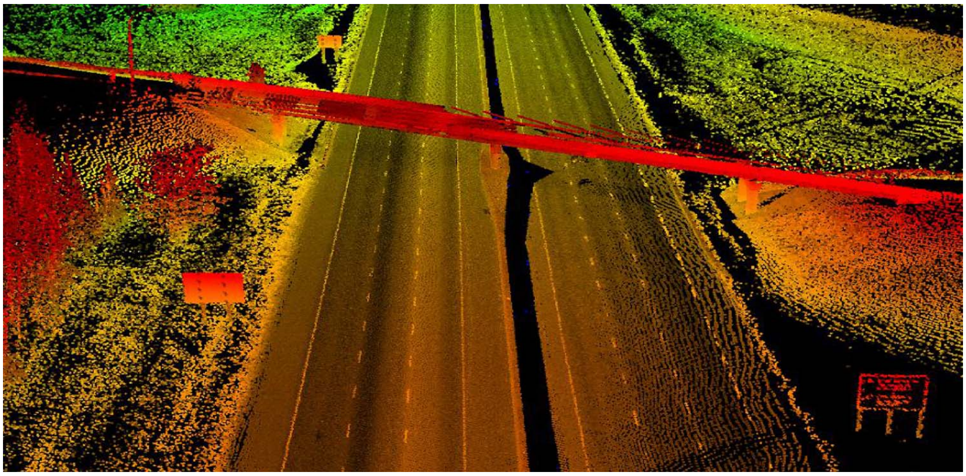

Fig. 1. LiDAR Point Cloud.

design guide recommends using 2.5 s for a driver's perception reaction time (PRT) and a deceleration value of 3.4 m/s^2 (AASHTO, 2011). Those deterministic values are typically percentile values which were empirically derived based on the performance of a sample of drivers. Therefore, although designing highways to meet SSD requirements defined in design codes might ensure that sufficient sight distance is available for most drivers, a significant portion of drivers, who have longer PRT or lower deceleration rates, might not find the available sight distance adequate. Although the proportion of drivers with limited abilities might currently be low, the fact that population demographics are changing (aging population) means that this will no longer be the case.

Statistics in Canada show that the average age of the driving population is on the rise with projections predicting that by 2030 around 20% of all drivers will be over the age of 65 (Road Safety Canada Consulting, 2011). A large portion of old drivers are typically slower in both their perception of risk and the manner in which they react to hazards on the road. This is due to many factors including reduced visual acuity, reduced flexibility and motion range, narrower field of vision, greater sensitivity to glare and reduced muscle strength. All these factors result in drivers having longer perception reaction time, hence, requiring longer sight distances.

Deceleration rate, is another factor that affects sight distance requirements on highways and one which may vary among drivers of different ages. Old drivers with limited abilities are less likely to apply similar pressure to brake pedals as young drivers, hence, occasional differences in deceleration rates may appear. Moreover, vehicle kinematics also differ among different vehicles. Furthermore, in places of adverse weather conditions surface traction might not always be best and result in reduction in deceleration rates. Similarly, deceleration rates might also be affected by pavement conditions or even tyre conditions.

Safety performance of old drivers has been researched in many studies (Marottoli et al., 1994; Foley et al., 1995; McGwin and Brown, 1999; Janke, 2001; Lyman et al., 2001; Jurewicz et al., 2017). In general, research has found that, despite their cautious driving habits, drivers aged 70 and older have the highest collision rates per kilometer driven when compared to other age groups except young male drivers (Li et al., 2003). Moreover, research has also shown that old drivers are at a higher risk to be killed when involved in a collision (Turcotte, 2015). The growing population of old drivers along with the fact that a large proportion of those drivers have limited abilities means that the overall population of drivers with limited abilities on our roads is expected to increase. As a result, it is extremely important that such a change is taken into account when assessing the safety of existing highways and when designing new highways, which is the motivation of research in this paper.

Whether it is human factors, deceleration rates or environmental conditions, all these factors affect how much sight distance is required by drivers on a highway segment. Although integrating all factors into design might not be economically feasible, changes in driver demographics might require slight changes to existing standards. Before that is done though, it is essential to understand whether or not existing highways are able to accommodate the anticipated changes.

This paper aims to investigate the extent to which sight distance on existing highways can accommodate variation in human factors, environmental conditions, and vehicle kinematics. Specifically, the paper aims to understand how changing those factors can impact the percentage of noncompliance in stopping sight distance on a road segment (i.e. the portion of the segment where sight distance requirements are not met).

First the paper adopts an algorithm which could be used to automatically compute the available stopping sight distance along a Light Detection and Ranging (LiDAR) point cloud model of the highway. LiDAR data is collected through laser scanners reflecting light beams off objects. The scanners are combined with Global Navigation Satellite System (GNSS) receivers and inertial measurement unit (IMU) which provide information about the exact position of the scanner. Constant scanning of objects around the sensor creates a 3D point cloud of known positional attributes illustrated in Fig. 1. LiDAR data on highways is often collected through Mobile Laser Scanning (MLS). In such practice scanning equipment is mounted on vehicles, which travel along the highway of interest capturing 360° imageries of the roadway.

Among many other applications in transportation and highway engineering (Holgado-Barco et al., 2014; Ai and Tsai, 2016; Gargoum et al., 2017b; Holgado-Barco et al., 2017; Gargoum et al., 2018a; Gargoum et al., 2018b; Gargoum et al., 2018c), the availability of LiDAR data makes it possible to assess sight distance on a road segment in a timely manner. The methodology applied in this paper is similar to that proposed in (Castro et al., 2013; Gargoum et al., 2018). The method creates a digital surface model of the highway with observer and target points defined along the road. Line of sight assessment is performed and the outputs are processed to calculate the available sight distance on the segment. This study fully automates the sight distance assessment procedure on LiDAR highways by writing a python code which can perform the analysis from multiple LiDAR highways without using the user interface in ArcGIS.

After computing the available sight distance along the highways of interest, the ASD is compared to the theoretical sight distance required while changing different variables in the sight distance equation. The percentage of noncompliance along a highway segment is then calculated for a range of perception reaction times and deceleration rates. In order to further explore the impacts of different levels of noncompliance on the safety of a road segment, collision records in the compliant and noncompliant regions of a given segment were compared.

2. Literature review

This section provides a review of the existing studies which have examined the factors affecting the different variables in the stopping sight distance equation with a focus on factors such as perception reaction time and deceleration rate. In addition, the section also explores how previous studies have analyzed the difference between available stopping sight distance on existing roads and the theoretical sight distance requirements.

2.1. Variables in sight distance equation

In an early study, which conducted a thorough review of factors affecting perception reaction time (PRT), Green (2000), identified *driver age*, *expectation of hazard*, and the *urgency of the hazardous situation* as the main variables. In case of driver age, the study concludes that older drivers have a longer PRT than younger drivers. However, the study states that in order to establish a sound relationship between aging and change in PRT, more controlled studies are required.

In case of the degree of expectation of various hazards, the same study divides the expectation into three levels (expected signals, common but uncertain signals and surprise intrusion). For expected signals such as break lights of a lead vehicle, the paper reports the mean perception reaction time of drivers typically ranges from 0.70 to 0.75 s. For common but uncertain signals such as brake lights of a vehicle ahead in traffic, it found that PRT was in the range of 1.2–1.35 s. Finally, for surprise intrusion such as animals running onto the road, Green (2000) concludes that the PRT typically increases to 1.5 s which is twice that of expected signals (0.75 s).

For the final factor affecting PRT, defined as the "urgency of the situation", Green (2000) found that the relationship between this factor and PRT is a U-shaped relationship such that at very short, and very long, time-to-collision correspond to long PRT. Unlike the values recommended by AASHTO, which represent the 85th percentiles, the estimates provided in Green's paper for perception reaction times are mean values estimated based on the outputs of other studies.

In a report by the National Cooperative Highway Research Program (NCHRP) investigating the impacts of human factors on design equations, Campbell (2012) explores the variation in PRT under favorable and unfavorable conditions and the effects of that on SSD. A number of drivers were asked to drive under those two conditions while being subject to unexpected roadway hazards. The mean PRT and deceleration rates for drivers were measured. The report defines favorable conditions (i.e. good visibility) for the PRT as driving during the daytime with the hazard being clearly visible and directly in the line of sight of the driver. During night-time, the report states that favorable conditions for the PRT include self-illuminated or retro-reflectorized hazards that are immediately recognizable and near the driver's line of sight. Unfavorable conditions (i.e. poor visibility) for the PRT in daytime consist of hazards that are hidden or camouflaged by the surrounding background, unreflectorized, not self-illuminated and initially off the line of sight of the driver. Furthermore, during night-time, unfavorable conditions for the PRT exist for low beam headlights with or without street lighting as well as if glare exists from oncoming vehicles. In good visibility, the mean PRT was estimated to be 1.6 s while, for poor visibility, it was 5.0 s.

In addition to PRT, the study also explores the effects of favorable and unfavorable conditions on deceleration rates. Favorable conditions (i.e. good traction conditions) were defined as straight road segments, dry or wet pavement, vehicle tyres in good condition, and the vehicle being a passenger car. Unfavorable conditions (i.e. poor traction conditions) were defined as conditions when the stopping requirement happens in a curve or downgrade and where surface conditions were poor. For good traction conditions a 5.4 m/s^2 deceleration rate was estimated while for poor traction conditions the rate was d 4.2 m/s^2.

Realizing that there is an element of uncertainty in some of the variables in design equations such as the equation of SSD, many researchers have attempted using reliability analysis to integrate uncertainties into safety analysis of sight distance on segments (Ibrahim and Sayed, 2011; Ibrahim et al., 2012). The principles applied in reliability analysis follow the limit states design approach where variables in the design equations are treated as random variables, which are expressed as probability distributions rather than constant values. In attempts to model the statistical distribution of PRT and deceleration rate, Ismail and Sayed (2009) used the perception reaction time and deceleration rate from various studies. The mean perception reaction time was found to be lognormally distributed with a mean of 1.5 s and a standard deviation of 0.4 s. Similarly, deceleration rate was assumed to follow a normal distribution with a mean of 4.2 m/s^2 and a standard deviation of 0.6 m/s^2. Several other studies reviewed by Ismail and Sayed (2009) estimated mean PRTs between 1.21 s and 1.4 s with standard deviations from 0.74 s to 0.15 s.

As evident in the review, variables used to predict required SSD on a highway segment vary depending on many factors. PRT is affected by visibility conditions, age, hazard expectancy and situation urgency. Similarly, surface conditions, the driver and vehicle driven all affect the deceleration rate. The next section explores the studies which have analyzed the difference between available stopping sight distance on existing roads and the theoretical sight distance requirements while taking variation in different variables in the sight distance equation.

2.2. Available sight distance

Gavran et al. (2016), studied the differences between available sight distance and theoretical sight distance while addressing the importance of integrating operating speed into sight distance assessment. The authors defined three types of sight distance. Available Sigh Distance (ASD) was defined as the sight distance available based on road geometry, theoretical Stopping Sight Distance (SSD) was defined as a mathematically derived using the SSD equation and a design speed, and Required Sight Distance (RSD) was defined as a theoretical value which was mathematically derived but using the operating speed. The aim of the paper was to propose means of measuring those types of sight distances on roads, particularly RSD, and plot them against one another. For RSD, the authors import lines of sight representing the RSD onto a triangulated a 3D model of the analyzed highway. Cross sections of the 3D model are then extracted along the sight lines to measure the RSD. To measure the ASD, a triangulated 3D model of the road was imported into a 3D CAD environment. The ASD was then plotted against the RSD. Although the authors do not provide much discussion of the results, it is mentioned that the ASD exceeded the RSD for most of the test segments.

SSD and the horizontal line of sight offset, when approaching a horizontal curve and within the horizontal curve, were also studied in (Wood and Donnell, 2014). These two cases (i.e. when approaching the curve and when driving on the curve) were investigated in six different theoretical combinations of speed limit, curve radius, and superelevation. Using previous speed prediction models and reliability theory, the probability of noncompliance was estimated. The probability of noncompliance was defined in this research as the probability of a driver not having sufficient SSD to perceive, react, and brake before reaching an object on the curve. The results showed that the probability of noncompliance when approaching the curve is greater than within the curve. This led the authors to suggest that the same SSD and line of sight offset should be used within the curve and near the end of the curve.

Sarhan and Hassan (2008) estimated the probability of noncompliance (referred as the probability of hazard) on a hypothetical roadway segment using a computer program. This computer program was developed to calculate and compare the available and required sight distances profiles in 2D and 3D. The program was used to estimate the probability of hazard on a horizontal curve with flat grade in a cut section and on horizontal curves combined with different crest and sag vertical curves. The results showed that the maximum probability of hazard value of all the cases was around 1%. The authors concluded that the deterministic approach of SSD was conservative in terms of safety, due to the low values of the probability of hazard, while this approach might be uneconomic from their point of view.

In general, most studies in the literature acknowledge that SSD requirements might vary among the driving population, however, not much has been done to assess the extent to which existing roads (i.e. roads designed based on deterministic design standards) take those variations into account. Hence, the aim of this paper is to evaluate the adequacy of the available sight distance on the existing roadways by comparing the available sight distance with the SSD requirements given the variation in drivers' capabilities and driving conditions.

3. Sight distance extraction procedure

In order to be able to measure available sight distance along multiple highway segments, a technique which could extract sight distance information in an efficient and timely manner was required. The technique employed in this study extracts sight distance information from LiDAR point cloud highway models. The procedure used in this paper is similar to that proposed in previous studies, see, for example (Castro et al., 2013; Gargoum et al., 2018), however, in this paper the procedure is fully automated and does not require using the ArcGIS's General User Interface (GUI). Moreover, the procedure helps run the assessment for multiple LiDAR segments simultaneously, making it possible to perform network-level assessment of sight distance.

The method first involves overlaying closely spaced points on the LiDAR highway segment. These are points of known coordinates aligned parallel to the road's axis and used to represent multiple observers and targets along the highway. After importing the points, sight lines are constructed between all pairs of observers and targets and the line of sight tool in ArcGIS is used to assess visibility between the points. Since ArcGIS is developed based on the Python Programming language, different features in ArcGIS can be utilized by writing different python scripts instead of using the program's GUI. In this paper, Python is used to automate the process of calling the tools used to perform the visibility assessment on the LiDAR segment. Once the outputs of this assessment are obtained, a MATLAB algorithm is used to calculate the available sight distance along the analyzed highway segment. The following outline provides details of each step in the extraction process.

3.1. Generating observer and target points

The first step of the extraction procedure involves the extraction of observer and target points whose trajectories are parallel to the road's axis. These points could be points collected in separate GPS surveys or as part of the LiDAR data collection process. In this study points representing the trajectory of the LiDAR data collection vehicle are used as observer and target points. These points are extracted from the LiDAR highway model by filtering the point cloud file based on scanner angle. MATLAB is used to first read the LiDAR file using the "readlas" function. The LAS file is saved as a MAT-file to speed up processing. The vehicle trajectory points (i.e. the points with angle zero that fall in the Nadir plane of the laser scanner) are filtered out and saved as separate *csv* files sorted by GPS time. These trajectory points are replicated with one set used as observer points (***I***) and the replicated set used as target points (***J***) as seen in Fig. 2. An observer height of 1.05 m and a target height of 0.38 m were used as recommended by the Alberta Highway Design Guide for stopping sight distance assessment (Alberta Infrastructure, 1999).

3.2. Digital surface model creation

The LiDAR data is represented as a point cloud and, therefore, it is necessary to build a Digital Surface Model (DSM) in the form of a raster surface representing the roadway. The raster surface is a grid of cells where the elevation of each cell is computed based on the average elevation of all the LiDAR points which fall in a particular cell. Once the DSM is created the observer and target points of known x, y, z coordinates are overlaid onto the surface.

3.3. Sight line construction and line of sight assessment

Once the observer and target points are imported and overlaid onto the raster surface, the Python code uses ArcGIS's ArcPy Python module to automate the construction of sightlines between pairs of observers and targets. This is done using the "Construct Sight Line" tool in ArcGIS. Similarly, ArcPy module is used to automatically assess the visibility from each observer to all targets using ArcGIS's "Line of Sight" tool as seen in Fig. 3. Alternatively, the "Construct Sight Lines" tool and the "Line of Sight" tool can both be used through ArcScene's GUI.

The "Line of Sight" tool works by assessing the visibility of all targets from the location of each observer, this assessment is performed along the sight lines created after running the "Construct Sight Lines" tool. For instance, to assess sight distance from observer *i,* the tool would assess the visibility on the sight lines connecting observer *i* to all targets in set ***J***. The tool works by testing for the intersection of the sight lines with the DSM raster surface. Any intersection between the sight line and the surface indicates that there is an object of higher elevation than the line, indicating that the target is not visible. Despite being able to assess obstructions along the sight line, the Line of Sight tool does not output available sight distance information. Instead, the "Line of Sight" tool outputs information about whether a target *j* is visible from an observer *i.* Fig. 4 depicts the outputs of the Line of Sight tool where a *TarIsVis = 1* indicates that the target is visible from observer with ID denoted as OID. In addition, the output also includes information about the length of the sight line (Shape_Length) between the observer and target that is unobstructed.

After constructing sight lines between pairs of observers and targets along the highway and assessing visibility along those sight lines, the python script exports the outputs from the "Construct Sight Line" and "Line of Sight" tools as *csv* tables. These output tables are then read into MATLAB for post processing to compute sight distance.

3.4. Available stopping sight distance computation

In order to compute the sight distance available along the segment, the outputs of the python code are analyzed using MATLAB. The MATLAB algorithm is written so that it loops through all target points (***J***) for each observer point (*i*) and checks the target visibility based on the outputs of the line of sight assessment discussed in the previous section. The algorithm finds the last visible target (*j*) from each observer; the distance between the observer and the last visible target is recorded as the available stopping sight distance for the observer. The flowchart in Fig. 5 shows a summary of the logic followed by the MATLAB algorithm to compute the ASD.

The algorithm takes into account that, at the end of the LiDAR segment (i.e. the end of the LAS file), the sight distance calculated will not be representative of the actual available sight distance since no point cloud data exist beyond the end of the segment. To address this, the algorithm was written so that it locates the last local maximum within each road segment (i.e. the last point towards the end of the segment where ASD exceeds SSD) and truncates (i.e. disregards) the computed available sight distance beyond this point. Unfortunately, this was a data limitation and to avoid such a problem (i.e. ASD dropping towards the end of the LiDAR segment) in the future, it is recommended that LiDAR data collected in surveys for sight distance

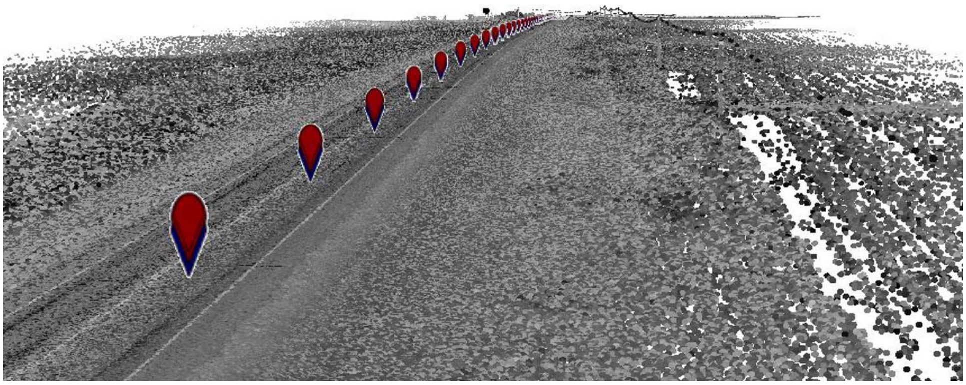

Fig. 2. Observer (Red) and Target (Blue) Points.

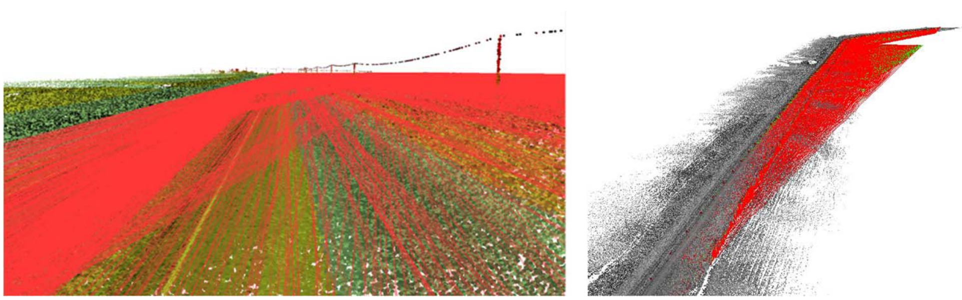

Fig. 3. Line of Sight Assessment.

analysis is stored in such a way to ensure the LAS files overlap towards the end of the LiDAR segment.

Once, the ASD is calculated along the LiDAR segment, the algorithm plots the available sight distance (ASD) as a function of distance along the roadway for all observer points along the road segment as seen in Fig. 6.

It is worth emphasizing that the method discussed in the last few sections was proposed in a recent paper by Gargoum et al. (2017a). In that paper the authors test the method on multiple highway segments while carefully assessing the locations of obstruction to validate the extraction procedure. The algorithm is also tested on a completely flat segment as means verifying that the algorithm was not prone to any false obstructions. Readers interested in more information about the validity of the method are referred to the said paper.

3.5. Stopping sight distance analysis

In addition to computing the available stopping sight distance for each observer point along the LiDAR segment, the MATLAB algorithm also computes the theoretical stopping sight distance using the

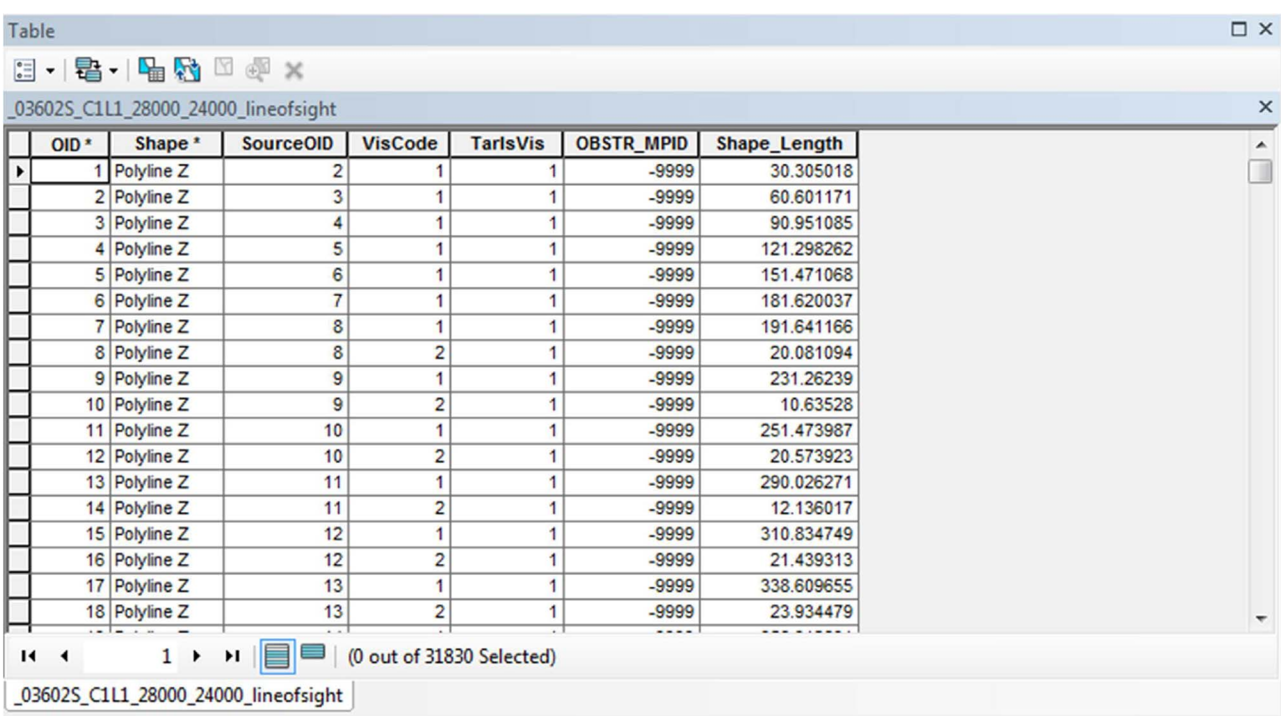

Table

_03602S_C1L1_28000_24000_lineofsight

OID *	Shape *	SourceOID	VisCode	TarIsVis	OBSTR_MPID	Shape_Length
1	Polyline Z	2	1	1	-9999	30.305018
2	Polyline Z	3	1	1	-9999	60.601171
3	Polyline Z	4	1	1	-9999	90.951085
4	Polyline Z	5	1	1	-9999	121.298262
5	Polyline Z	6	1	1	-9999	151.471068
6	Polyline Z	7	1	1	-9999	181.620037
7	Polyline Z	8	1	1	-9999	191.641166
8	Polyline Z	8	2	1	-9999	20.081094
9	Polyline Z	9	1	1	-9999	231.26239
10	Polyline Z	9	2	1	-9999	10.63528
11	Polyline Z	10	1	1	-9999	251.473987
12	Polyline Z	10	2	1	-9999	20.573923
13	Polyline Z	11	1	1	-9999	290.026271
14	Polyline Z	11	2	1	-9999	12.136017
15	Polyline Z	12	1	1	-9999	310.834749
16	Polyline Z	12	2	1	-9999	21.439313
17	Polyline Z	13	1	1	-9999	338.609655
18	Polyline Z	13	2	1	-9999	23.934479

1 (0 out of 31830 Selected)

_03602S_C1L1_28000_24000_lineofsight

Fig. 4. Line of Sight Outputs.

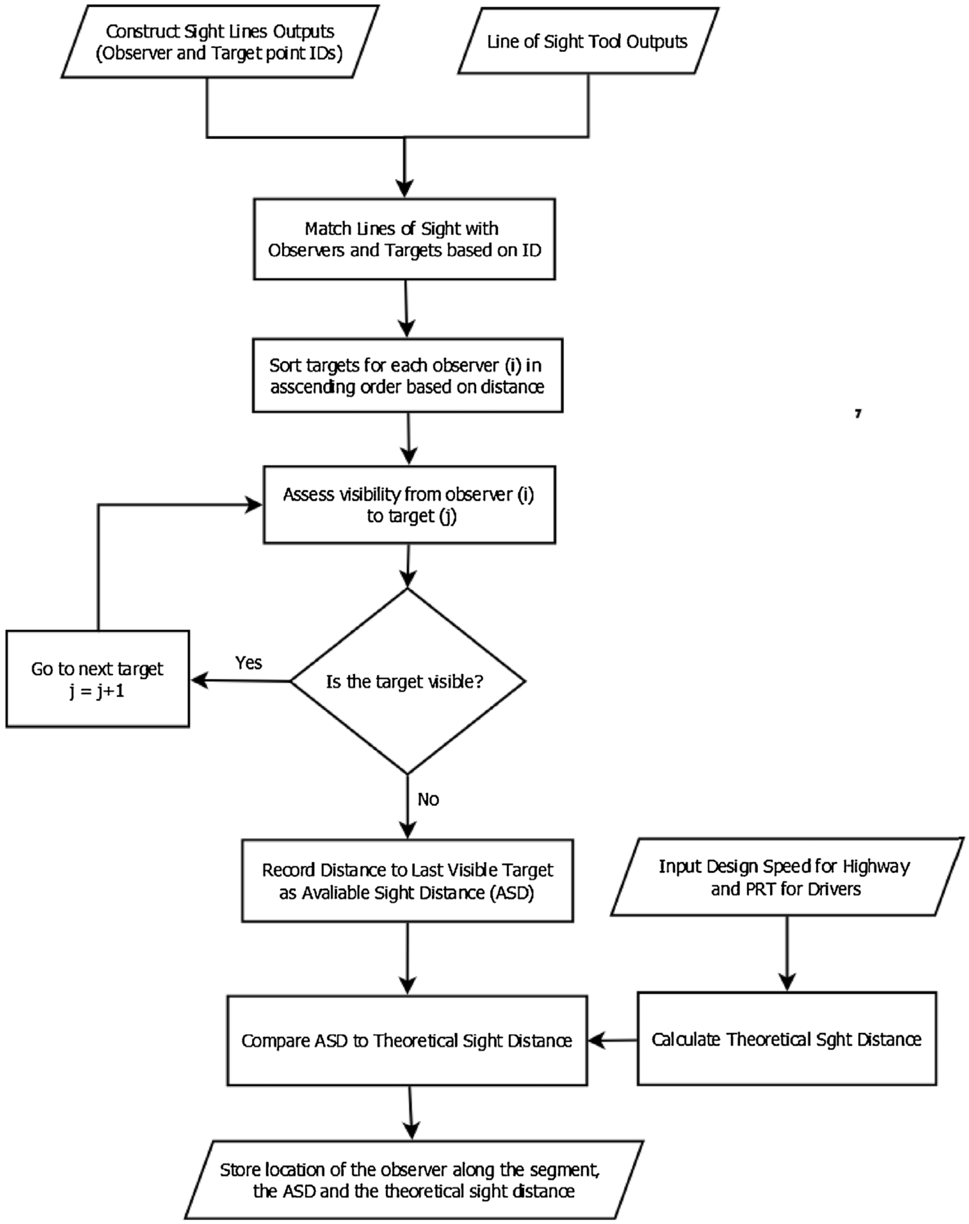

Fig. 5. Available Sight Distance Computation.

following stopping sight distance equation, which is used to compute SSD in AASHTO's highway design guide and Alberta's Highway Design Guide (Alberta Infrastructure, 1999; AASHTO, 2011).

$$SSD = 0.278Vt + \frac{V^2}{254(\frac{a}{g} \pm G)}$$

where, V [km/h] denotes the design speed of the highway, t [sec] is the perception reaction time of the driver (AASHTO recommends using 2.5 s), a [m/s^2] is the deceleration rate of the vehicle (AASHTO recommends using a deceleration rate of 3.4 m/s^2), g [m/s^2] is the gravitational acceleration (9.81 m/s^2) and G [%] is the grade of the highway (3% downgrade is used for tabulated SSD values in AASHTO).

When using the equation, the MATLAB code uses a range of values for perception reaction time and deceleration rate to calculate different thresholds for the minimum allowable stopping sight distance on a segment. Based on the different thresholds the MATLAB algorithm computes the percentage of each road segment that is noncompliant with theoretical design stopping sight distances (i.e. the length of the segment where the available stopping sight distance is less than the theoretical stopping sight distance as a ratio of the total length of the segment).

4. Case study

In this paper, the primary aim was to assess the extent to which existing highway segments meet stopping sight distance requirements while taking into account variations in human factors and other variables. This was achieved by comparing the available stopping sight distance on several crash prone highway segments in the Province of Alberta, Canada to the theoretical (required) stopping sight distance. Three different levels for the required stopping sight distance were computed while changing the values of the perception reaction time and deceleration rate. The next subsection defines the ranges used for both variables to calculate the required SSD. Moreover, Section 4.2 provides information about the highway segments on which the assessment was performed.

4.1. Variation in human factors

The range of perception reaction time (PRT) and deceleration rate

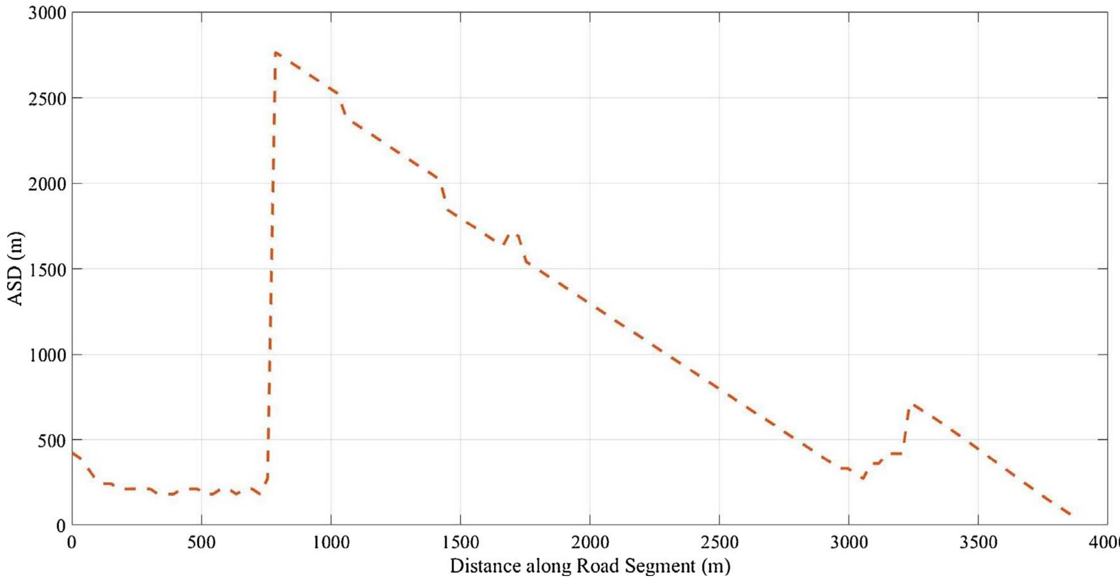

Fig. 6. Sample of ASD Plot along a Segment of Highway 20, AB, Canada.

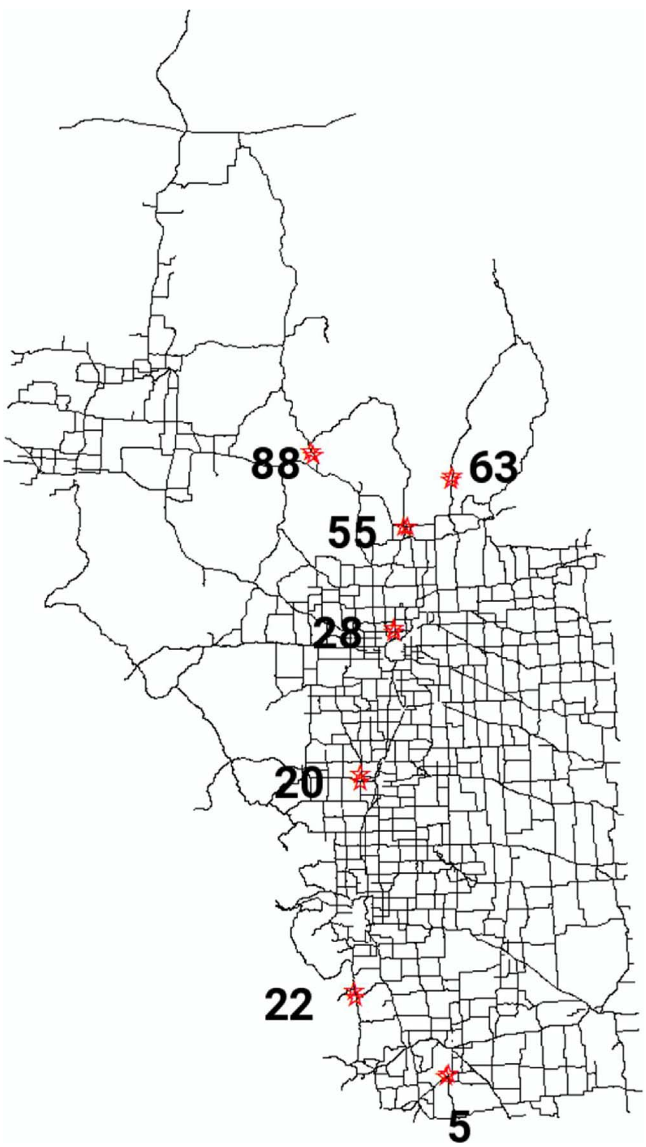

Fig. 7. Test Locations.

used to calculate SSD were defined based on the outputs of previous studies discussed in the literature review. For perception reaction time, two levels were defined based on driver capabilities and driving conditions. Drivers with limited ability who are driving in poor conditions were assumed to have long PRT. In contrast, highly skillful drivers with high cognitive skills driving in clear conditions were assumed to have very short PRT. In order to be consistent with the PRT values defined in the literature, a short PRT was assumed to be 1.6 s and a long PRT was assumed to be 5.0 s (Campbell, 2012). It is worth noting here that these values were previously defined in research conducted under the NCHRP and published by the Transportation Research Board (TRB) in a report titled "*Human Factors Guidelines for Road Systems*" (Campbell, 2012).

Similar to PRT, for deceleration rate, two levels were defined. Deceleration rate under poor conditions was defined as conditions where a driver only applied slight pressure to the brake pedal and where surface traction conditions were poor. Deceleration rate under good conditions, on the other hand, is when a driver applies severe pressure to the brakes and where surface traction is good. For these two conditions deceleration rates of 5.4 m/s^2 and 3.4 m/s^2 were used for good and poor conditions, respectively (Campbell, 2012).

Theoretical SSD was calculated based on the conditions defined in the previous paragraphs. For skillful drivers with high cognitive skills driving in ideal conditions, SSD was calculated based on a PRT of 1.6 s and a deceleration rate of 5.4 m/s^2 (best case SSD). For old drivers with limited skill and low cognitive ability, SSD was calculated using a PRT of 5.0 s and a deceleration rate of 3.4 m/s^2 (worst case SSD). In addition to the SSD values which take into account variations in driving conditions and human factors, the SSD based on AASHTO's recommendation (PRT = 2.5 s and Deceleration rate = 3.4 m/s^2) was also calculated. The ASD plots as well as the percentage of the road segment that does not meet SSD for each of the three levels (best, worst case or AASHTO) are all computed in MATLAB. It is worth noting that the SSD requirements under the worst-case condition (top/red horizontal line in Fig. 8) rise above AASHTO's SSD threshold (bottom/blue horizontal line in Fig. 8) by 25–30%, depending on the design speed of the road.

4.2. Test segments

The extraction procedure was applied on seven different crash prone highway segments in the Province of Alberta, Canada. All highway segments were 2-lane undivided rural segments with a speed limit of 100 kph. The length of the test segments ranged from 2.5 km on

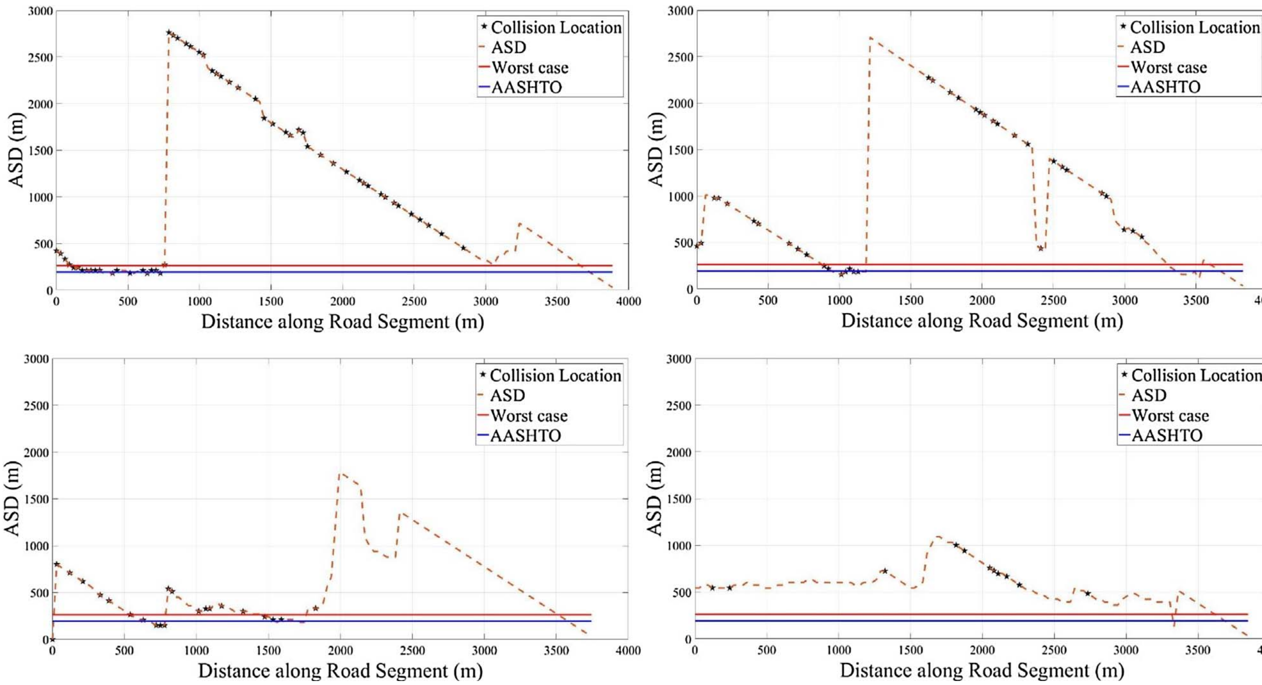

Fig. 8. Plots Samples of the ASD with the different SSD Cases for Segments of Highways 20 (Top Left), 28 (Top Right), 55 (Bottom Left), and 88 (Bottom Right). Note: y-axis represents available sight distance (ASD) in meters and x-axis represents the distance along the segment in meters. (For interpretation of the references to colour in the text, the reader is referred to the web version of this article).

Table 1
Geometric and Traffic Information on Test Segments.

Highway	Total Length (km)	AADT (veh/day)	Heavy Vehicles (%)
5	6.219	4535	6.9
20	9.554	8755	6.45
22	9.661	4403	9.58
28	5.334	7270	5.2
55	3.957	4893	8.73
63	2.514	3988	27.63
88	6.363	2340	27.73

highway 63–9.55 km on highway 20. The average length of all segments was 6.23 km. The seven highways were spread across different parts of the province as seen in Fig. 7. Table 1 shows a summary of information on the length and traffic information on the seven test segments.

4.2.1. Crash prone locations

In the first stage of the Safety Management Process, *Network Screening* is used to identify crash prone locations. This involves identifying locations that are deemed unsafe and ranking those locations based on the potential for crash reduction. The literature includes several methods to identify and rank these locations as part of the network screening process. Common methods include comparing crash frequencies, crash rates, or using the Empirical Bayes (EB) method. Among the different crash identification and ranking methods, the EB method is considered to be the most consistent crash prone identification method and provides the most reliable results when compared to the other methods (Montella, 2010).

In brief, the EB method combines the observed number of crashes and the estimated number of crashes to provide an unbiased prediction of the true safety at a location. The observed number of crashes is usually extracted from historical crash data. The estimated number of crashes is computed from sites with similar traffic and geometric characteristics to the sites being analyzed using crash prediction models. The sites are then ranked using the EB method, where sites with higher EB values will have more potential for safety improvement.

Among 17,355 two-way two-lane segments in the Province of Alberta, the top crash prone locations were selected for the assessment in this study. These locations include segments of highways 5, 20, 22, 28, 55, 63, and 88.

4.2.2. LiDAR data

LiDAR data along the crash prone highway segments was collected by Alberta Transportation using a third-party service. The data was collected using RIEGL VMX-450 Mobile Laser Scanning (MLS) system. The MLS system is mounted to a data collection truck and is able to collect data as the truck travels down the highway at highway speeds. The system is equipped with two VQ-450 scanners which have a scan rate of up to 1.1 million points per second and a scan speed of 400 lines per second (Riegl, 2015). The density of the points on a scanned object depends on the range, and the speed of the data collection truck. Provincial surveys conducted at 90 km/h result in LiDAR point densities on the pavement surface of 150–1000 points/m^2 (Steel et al., 2014).

5. Results and discussion

Fig. 8 shows samples of the plots produced by the MATLAB algorithm which display the ASD for the test segments. The y-axis on the plots represents the available sight distance and the x-axis represents the distance along the segment. In addition to the available sight distance, two different horizontal lines are drawn across the plots representing the SSD requirements under worst case and AASHTO. If at any point along the segment the ASD falls below one of the horizontal lines this indicates that SSD requirements are not met at that location.

For all the highway segments analyzed, the ASD rarely dropped below the sight distance requirements under best conditions (i.e. the threshold defined for drivers with short PRT, high skill and high cognitive ability). Accordingly, the discussion of the results presented in the next few subsections will focus on whether or not ASD meets the AASHTO requirements and the worst-case sight distance requirements defined for drivers with limited skills and low cognitive ability (i.e. sight distance requirements that take limitations in human factors into

Table 2
Noncompliance Rates Compared.

Highway	Worst Case			AASHTO		
	Length of NC[a] Region (m)	Total Length (m)	Percent NC (%)	Length of NC Region (m)	Total Length (m)	% NC (%)
5	260.2	6218.6	4.185	61.2	6218.6	0.984
20	1928.2	9554.1	20.181	630.8	9554.1	6.602
22	1054.4	9661.1	10.914	60.5	9661.1	0.626
28	513.3	5334.8	9.621	332.7	5334.8	6.236
55	694.8	3957.4	17.557	143.3	3957.4	3.622
63	393.5	2514.2	15.651	91.1	2514.2	3.625
88	30.4	6363.4	0.477	0.0	6363.4	0.000
Average	696.4	6229.1	11.2	188.5	6229.1	3.1

[a] NC: Noncompliance/Noncompliant.

account).

5.1. Non-compliance rates

Table 2 presents the total length of each of the analyzed highway segments and the portion of that length where SSD requirements were not met (i.e. the length of the noncompliant regions). The ratio of the length of the noncompliant region to the total length of each segment (i.e. percent noncompliance) is also computed and shown in the table. The results are shown for the SSD requirements under AASHTO and under the worst case.

5.1.1. Worst case

When human factors are integrated into the analysis (i.e. when the ASD is compared to the threshold which takes human factors into account) the results show that a substantial portion of the analyzed segments do not meet sight distance requirements. On 5 of the 7 analyzed segments noncompliance rate exceeds 9.62% with an average of 14.8% for the 5 segments. When considering all 7 segments average percent noncompliance drops to 11.2%. As seen in Fig. 9, Highways 20 and 55 had the highest noncompliance rates. The percent noncompliance on Highway 20 was 20.2%. In terms of actual length, this translates to almost 2 km of the 9.6 km analyzed not meeting the sight distance requirements. On Highway 55, noncompliance percent was 17.6% (almost 700 m of the 4 km analyzed).

Highway 88 was the highway with highest compliance rates. On this highway, sight distance requirements, while accounting for human factors, were met on all but 30 m of the segment (i.e. only 30 m of the 6.3 km analyzed were noncompliant). The segment with the second lowest percent noncompliance is Highway 5 where only 4.2% of the analyzed 6.2 km did not meet sight distance requirements.

These numbers show that the ability of existing highways to accommodate drivers with low skills and low cognitive ability such as old drivers is restricted to only 80–85% of the road. In other words, those drivers spend 15–20% of their time driving on highways that are not designed to meet their needs, which puts them under an additional risk.

5.1.2. AASHTO

When compared to AASHTOs theoretical SSD requirements, the highest rate of noncompliance on the analyzed segments was 6.6%. This was observed on Highway 20. On average, percent noncompliance on the analyzed segments with respect to AASHTO was 3.1%. This is reasonable considering the fact that highways are designed to meet AASHTOs SSD requirements (Alberta Design Guide recommends the same guidelines as AASHTO for SSD calculations). Out of the 7 crash prone highway segments analyzed, Highway 88 was the only highway that was perfectly compliant to AASHTO's sight distance requirements as evident in Fig. 10, although it is worth pointing out that the analyzed segments of Highway 5 and Highway 22 also had low noncompliance rates of 0.98% and 0.6%, respectively.

5.2. Safety analysis

As evident by the results presented in the previous section, a substantial portion of the analyzed highway segments do not meet stopping sight distance requirements, when human factors and driving conditions are taken into account. In fact, the analysis shows that even AASHTO sight distance requirements were not met on some portions of the analyzed segments. To understand the impacts of such design deficiencies on safety, crash rates at locations of noncompliance were compared to crash rates on compliant regions on each of the analyzed segments. This process is known as the *Diagnosis Stage* of the Safety Management Process, in this stage different tools are used to analyse trends in the crash data before deciding on an appropriate countermeasure to treat the problem. Unlike the network screening stage where the EB method has been identified as the most accurate method, the Highway Safety Manual does not recommend a specific method for the diagnosis of crash sites.

Since the same traffic volume travels through both the compliant region and the noncompliant region of the same highway segment,

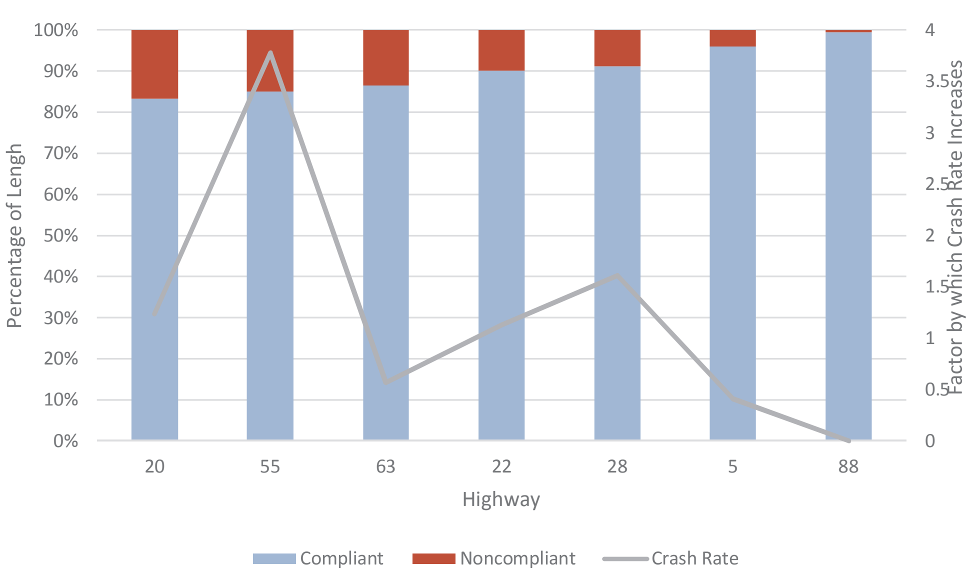

Fig. 9. Percent Compliance/Noncompliance and Corresponding Change in Crash Rates (Worst-Case).

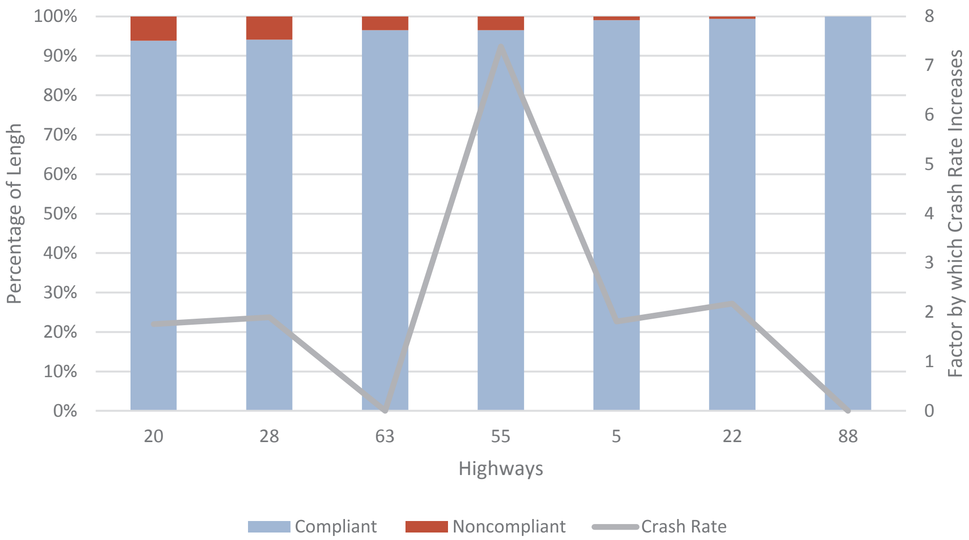

Fig. 10. Percent Compliance/Noncompliance and Corresponding Change in Crash Rates (AASHTO).

crash rates per length were used to compare safety at the two regions. Crash rates were calculated based on the collision data from 2009 to 2014. Moreover, the types of collisions and the demographics of drivers involved in collisions which occurred at locations of noncompliance were also explored to identify any links between design deficiencies and safety. Before discussing the results of the assessment, it is worth noting that SSD requirements under the worst-case condition rise above AASHTO's SSD threshold by 25–30%, depending on the design speed of the road.

5.2.1. *Crash rates*

Table 3 shows the crash rates (crashes per km) on the analyzed highway segments for the noncompliant and the compliant regions. The table also shows the change in crashes in the two regions expressed as a ratio and a percentage. As evident in the table, it is clear that on segments where non-compliant regions exist, these regions typically experience higher crash rates than compliant regions for both AASHTO and Human Factor analyses. It is important to note here that the results presented in this paper only examine the existence of a correlation between limitations in sight distance and changes in crash rates. The causal relationship between the two can only be explored if other confounding factors affecting crashes are accounted for, which is out of the scope of this paper. That being said, the comparison of crash rates on compliant and noncompliant regions of the same segment does help account for many confounding factors including geometric information such as number of lanes, lane widths, shoulder widths, pavement conditions, traffic volumes and many other factors.

5.2.1.1. Worst case. When considering all analyzed crash prone segments, on average, the noncompliant regions when driver limitations are considered experience crash rates 24.8% higher than compliant regions. For crash prone segments where the percent noncompliance was higher than 9.6% (i.e. more than 9.6% of the length of the segment was noncompliant), crash rates in the noncompliant region were found to be higher than those in the compliant regions on all but one of the five segments. On average, for those highways, the noncompliant region experiences a crash rate that is 66.5% higher than that of the compliant region. The highest increase in crash rates was observed on Highway 55. For this highway, the crash rate increases from 15.6 crashes per km in the compliant region to 59 crashes per km in the noncompliant region (that is almost 4 times the crash rate). Highways 20 and 28 were also segments where there was a substantial increase in crash rates in the regions where sight distance did not meet the theoretical requirements when taking human factors into account (i.e. regions of noncompliance). The increase was 23% and 61% for highways 20 and 28, respectively. Highway 63 was the only segment, of those analyzed, where crash rates were not higher in the noncompliant regions despite a relatively high percent of noncompliance. This could be down to the fact that only 2.5 km of Highway 63 were analyzed (the shortest segment out of all highways).

In general, the findings demonstrate that when portions of a highway segment are noncompliant to sight distance requirements which take limitations in driver abilities into account, it is likely that those portions of a highway will experience higher crash rates. Considering the fact that the population of drivers with limited abilities is on the rise, this finding is quite concerning.

5.2.1.2. AASHTO. When considering any part of a segment that does

Table 3
Crash Rate Analysis.

	Worst Case				AASHTO			
Highway	NC-CR[a]	C-CR[b]	Ratio (NC to C)	% Change	NC-CR	C-CR	Ratio (NC to C)	% Change
5	7.69	18.63	0.41	−58.7	32.67	18.03	1.81	81.2
20	42.53	34.36	1.24	23.8	60.24	34.29	1.76	75.7
22	8.54	7.55	1.13	13.0	16.54	7.60	2.17	117.5
28	33.12	20.53	1.61	61.3	39.08	20.59	1.90	89.8
55	59.01	15.63	3.77	277.5	139.54	18.88	7.39	639.2
63	5.08	8.96	0.57	−43.3	0.00	8.67	0.00	−100.0
88	0.00	6.32	0.00	−100.0	0.00	6.29	0.00	−100.0
Average	22.28	16.00	1.25	24.80	41.15	16.34	2.15	114.76

[a] NC-CR: Noncompliant Crash Rate in Crashes/km.
[b] C-CR: Compliant Crash Rate in Crashes/km.

Table 4
Age Distribution of All Drivers Involved in Crashes.

Highway	All Drivers				Male Drivers Only			
	Noncompliant Region		Compliant Region		Noncompliant Region		Compliant Region	
	Under 70	Over 70	Under 70	Over 70	Under 70	Over 70	Under 70	Over 70
5	4	0	302	23	2	0	159	17
20	324	6	1541	27	201	6	765	16
22	17	0	139	4	14	0	99	4
28	47	6	515	12	40	6	362	10
55	103	8	195	10	52	6	65	8
63	129	5	744	10	112	5	633	10
88	0	0	75	3	0	0	53	3
Total	624	25	3511	89	421	23	2136	68
Proportions		0.0385		0.0274		0.052		0.031

not meet AASHTO's SSD requirements as noncompliant the results are even more concerning. Although regions of noncompliance under AASHTO are short (i.e. the range from 0% to 6.6%), regions of noncompliance experience significantly higher crash rates. Out of the 7 highways analyzed, 5 highways had higher crash rates in regions that were not compliant to AASHTO's SSD requirements. In fact, on those 5 highways noncompliant regions experienced a crash rate which was, on average, 2.95 times higher than that in compliant regions. For the other two highways, Highway 88 meets AASHTO's SSD throughout (i.e. there were no noncompliant regions) and no crashes were recorded in the noncompliant regions on Highway 63. The highway which experienced the highest increase in crash rates in its noncompliant region compared to its compliant region is Highway 55. This highway was also the one with the highest increase in crash rates in its noncompliant region when considering sight distance requirements under the worst case.

When comparing the changes in crash rates between the noncompliant and the compliant regions, it is noted that, despite being shorter, noncompliant regions under AASHTO experience higher increases in crash rates when compared to noncompliant regions under the worst case SSD requirements. In other words, when the available sight distance dropped below AASHTO's sight distance threshold, the crash rate increase was more critical than when the ASD dropped below the worst-case threshold. This is highly intuitive considering that drops in ASD below the worst-case threshold only affect drivers with limited abilities. In contrast to that, drops in ASD below AASHTO's requirements affect more drivers. In fact the findings are in contrary to previous research where no correlation between SSD and crashes (all types, all severities) was found for up to 30% deficiency with respect to the AASHTO design guidelines (Fambro et al., 1997; Jurewicz et al., 2017).

To further verify the impacts of limitations in SSD on safety, a Chi-Squared test of association was used. The test was used to assess whether there was statistical correlation between a region being noncompliant to SSD requirements and crash rates increasing in that region. The tests revealed that the association was statistically significant at the 10% level with p-values for the likelihood ratio of 0.08 (for AASHTO's case) and 0.104 (in case of the worst case).

The more critical observations when AASHTO's requirements were violated are even more alarming when taking the ageing population into consideration. Currently, not many drivers have a longer perception reaction time (i.e. the majority of drivers today are comfortable driving on roads designed to meet AASHTO's sight distance requirements). When ASD drops below AASHTO's requirements, even for short periods, a large population of drivers is affected, which is reflected by the substantial increase in crash rates. The ageing population means that, over the next few years, more drivers will fall in the category of drivers with limited abilities, hence, drops in ASD below the SSD requirements which integrate driver ability and human factors will affect more drivers and the consequences will potentially be more critical, than the increases observed in this paper.

Based on the outputs of the analysis performed in this study and the projections that predict increases in the ages of the driving population, over 10% of existing highways won't satisfy the needs of 20% driving population (Statistics Canada predicts that by 2030 20% of the driving population will be over 65). This finding is highly critical to future design of highways. Given the fact that the majority of developed countries have aging populations, authorities responsible for highway design must take such figures into consideration when designing new roads and when upgrading existing highways or when setting new speed limits.

5.2.2. *Age structure*

To get more insight into whether drivers with limited abilities are overrepresented in the noncompliant regions, the age distribution of individuals involved in crashes which happened in the noncompliant region was compared to those that occurred in the compliant region on all the analyzed highway segments. It is important to emphasize here that dividing the segments into compliant and noncompliant sections was based on a PRT of 5 s, as previously defined. This does not mean that all crashes that occurred in the noncompliant regions were because the drivers had a PRT of 5 s or more, instead it is only a threshold used to divide the segments into portions of low ASD and high ASD. It is also worth stressing that, the reason 5 s threshold was adopted is because that was previously defined in research conducted under the NCHRP and published by the TRB in the report titled "Human Factors Guidelines for Road Systems" (Campbell, 2012).

Table 4 splits the number of drivers involved in crashes for the compliant and noncompliant regions into drivers above 70 and below 70. The table also shows the proportion of drivers over 70 in the compliant and the noncompliant regions. As seen in the table, when considering all seven of the analyzed highway segments, it is noted that the proportion of drivers over 70 who were involved in crashes in noncompliant regions (prop = 0.0385) is higher than that in compliant region (prop = 0.0274).

In an attempt to identify whether this difference was statistically significant, a test of proportions was run between the two samples. For more information about the test the reader is referred to (Dixon and Massey, 1969; Garber and Hoel, 2014). The results of running the test revealed that the higher proportion of drivers over 70 in the noncompliant region was indeed statistically significant at the 90% confidence level (*p-value* = 0.06).

To further analyse the data, drivers were divided into two groups based on gender. Table 4 also shows the proportions for male drivers only. As seen in the table, the proportion of drivers over 70 in the noncompliant regions was, again, higher than that in the compliant regions. Statistical testing of the difference of proportions for male drivers revealed that the difference was statistically significant at a 99% confidence level (*p-value* = 0.01). When female drivers were analyzed separately, there was not enough statistical evidence that the proportion of drivers over 70 was higher in the noncompliant region, however, statistical significance at the 95% confidence level was observed when the drivers were divided into over 75 and under 75 age groups (*p-value* = 0.04). Overall, male drivers are usually more aggressive than female drivers and hence have higher collision involvement. In Alberta, Transportation Traffic Collisions Statistics show that 4.9% of males over 65 are involved in collisions compared to only 2.7% of females (Alberta Transportation, 2014).

In general, the results indicate that old drivers could be at a higher risk of collision in regions of a segment where limitations in sight distance are more prevalent. In other words, regions of highways which are not designed to account for the limited skills and the low cognitive abilities of over-age drivers may subject those drivers to a higher collision risk. This finding is perfectly consistent with previous research which found that drivers over 70 years of age are at a higher risk of collision compared to other age groups (Li et al., 2003). In fact, the findings in this paper show that those drivers actually have a relatively low collision risk when driving on roads which take their limited abilities into account. This means that if roads were designed to accommodate those drivers this would help decrease their collision risk.

Although redesigning existing highways may not be feasible, the finding of this study must be taken into account when designing new highways. For existing highways, alternative approaches may be adopted on segments with high noncompliance rates to accommodate drivers with limited ability. For instance, speed limits on those roads may be revised to account for such information or, instead, variable speed limits could be used to accommodate drivers in regions of noncompliance. Based on the finding of this study, regions of noncompliance can extend up to 0.6 km, hence using variable speed limits could be an option. Connected Vehicles technology is also another factor which could help significantly in accommodating drivers with limited abilities. Vehicle to Infrastructure (V2I) communication could provide drivers with an advanced warning on the existence of a potential hazard, providing them with more time to react.

6. Conclusions and recommendations

This paper assesses the extent to which existing roads are able to accommodate stopping sight distance requirements while considering variations in human factors and driving conditions. The paper first develops an automated algorithm to evaluate the available sight distance on crash prone highways in the province of Alberta using remotely sensed LiDAR data. The available sight distance on each of those highways is then compared to the theoretical SSD requirements at three different levels (AASHTO, best conditions and worst case) and the percentage of the segment that is non-compliant to SSD requirements (i.e. the extent to which the analyzed segment meets SSD requirements) is analyzed. Worst-case sight distance requirements were defined for drivers with limited abilities driving in poor conditions, while best conditions represented drivers with high skill and high cognitive ability driving in good conditions. For the worst case, it was found that ASD fell below the required SSD requirements for up to 20% of the length of the tested segments, while for AASHTO the percent noncompliance reached 6% on some of the segments. Such an observation indicates that high noncompliance rates are expected anywhere between a PRT of 2.5 s and 5 s.

The safety analysis conducted in the study revealed that, in general, regions of noncompliance had significantly higher crash rates per km when compared to compliant regions of the same segment. Furthermore, the analyses revealed that old drivers (over the age of 70) were overrepresented in crashes occurring in noncompliant regions compared to crashes in the compliant regions. This difference was statistically significant particularly among male drivers.

The results obtained from the analysis show that portions of existing highways cannot accommodate a driving population with limited capabilities. Moreover, the results also show a link between design deficiencies on existing roads and crash occurrences, particularly when considering the age of the driving population. This is an extremely concerning matter that must be addressed in order to avoid future problems which could arise with the anticipated growth in the ages of the driving population. Accordingly, road authorities can use finding of this study and similar work to understand the extent to which design guidelines must be updated to accommodate changes in driving population when designing new roads. Furthermore, authorities can also consider the means by which limitations on existing highways could be addressed.

Acknowledgments

The authors would like to thank Alberta Transportation for sponsoring and providing the data used in this study. Acknowledgments are also extended to Alberta Innovates and Alberta Advanced Education for the financial support.

References

Aashto, 2011. Policy on geometric design of highways and streets. American Association of State Highway and Transportation Officials, Washington, DC 1 (990), 158.
Ai, C., Tsai, Y.J., 2016. An automated sign retroreflectivity condition evaluation methodology using mobile lidar and computer vision. Transp. Res. Part C Emerg. Technol. 63, 96–113.
Alberta Infrastructure, 1999. Highway Geometric Design Guide. Transportation. A. ed., Alberta.
Alberta Transportation, 2014. Alberta traffic collision statistics 2014. Safety. A.T.O.O.T. ed.
Campbell, J.L., 2012. Human Factors Guidelines for Road Systems Transportation Research Board.
Castro, M., Anta, J.A., Iglesias, L., Sánchez, J.A., 2013. Gis-based system for sight distance analysis of highways. J. Comput. Civ. Eng. 28 (3), 04014005.
Dixon, W.J., Massey, F.J., 1969. Introduction to Statistical Analysis McGraw-Hill. New York. .
Fambro, D.B., Fitzpatrick, K., Koppa, R.J., 1997. Determination of Stopping Sight Distances Transportation Research Board.
Foley, D.J., Wallace, R.B., Eberhard, J., 1995. Risk factors for motor vehicle crashes among older drivers in a rural community. J. Am. Geriatr. Soc. 43 (7), 776–781.
Garber, N.J., Hoel, L.A., 2014. Traffic and Highway Engineering Cengage Learning.
Gargoum, S., El-Basyouny, K., Sabbagh, J., 2018a. Assessing stopping and passing sight distance on highways using mobile lidar data. J. Comput. Civ. Eng.
Gargoum, S.A., El-Basyouny, K., Sabbagh, J., Froese, K., 2017b. Automated highway sign extraction using lidar data. Transp. Res. Rec. J. Transp. Res. Board 2643, 1–8.
Gargoum, S., El-Basyouny, K., Froese, K., Gadowski, A., 2018a. A fully automated approach to extract and assess road cross sections from mobile lidar data. IEEE J. Trans. Intell. Transp. Syst. (IEEE Xplore Edition).
Gargoum, S., Karsten, L., El-Basyouny, K., 2018b. Network level clearance assessment using lidar to improve the reliability and efficiency of issuing over-height permits on highways. Transp. Res. Rec. J. Transp. Res. Board 2643, 1–8.
Gargoum, S.A., El-Basyouny, K., Sabbagh, J., 2018c. Automated extraction of horizontal curve attributes using lidar data. Transp. Res. Rec. J. Transp. Res. Board.
Gavran, D., Fric, S., Ilić, V., Trpčevski, F., 2016. Sight distance analyses in road design process: Serbian practice. Transport 31 (2), 250–259.
Green, M., 2000. How long does it take to stop? Methodological analysis of driver perception-brake times. Transp. Hum. Factors 2 (3), 195–216.
Holgado-Barco, A., Gonzalez-Aguilera, D., Arias-Sanchez, P., Martinez-Sanchez, J., 2014. An automated approach to vertical road characterisation using mobile lidar systems: longitudinal profiles and cross-sections. ISPRS J. Photogramm. Remote Sens. 96, 28–37.
Holgado-Barco, A., Riveiro, B., González-Aguilera, D., Arias, P., 2017. Automatic inventory of road cross-sections from mobile laser scanning system. Comput.- Aided Civ. Inf. Eng. 32 (1), 3–17.
Ibrahim, S.E.-B., Sayed, T., 2011. Developing safety performance functions incorporating reliability-based risk measures. Accid. Anal. Prev. 43 (6), 2153–2159.
Ibrahim, S.E., Sayed, T., Ismail, K., 2012. Methodology for safety optimization of highway cross-sections for horizontal curves with restricted sight distance. Accid. Anal. Prev. 49, 476–485.
Ismail, K., Sayed, T., 2009. Risk-based framework for accommodating uncertainty in highway geometric design. Can. J. Civ. Eng. 36 (5), 743–753.
Janke, M.K., 2001. Assessing older drivers: two studies. J. Saf. Res. 32 (1), 43–74.
Jurewicz, C., Makwasha, T., O'callaghan, N., 2017. Verification of Austroads Road Design Criteria Based on Objective Safety Evidence Austroads Ltd. Sydney NSW 2000 Australia. .
Li, G., Braver, E.R., Chen, L.-H., 2003. Fragility versus excessive crash involvement as determinants of high death rates per vehicle-mile of travel among older drivers. Accid. Anal. Prev. 35 (2), 227–235.
Lyman, J.M., McGwin, G., Sims, R.V., 2001. Factors related to driving difficulty and habits in older drivers. Accid. Anal. Prev. 33 (3), 413–421.
Marottoli, R.A., Cooney, L.M., Wagner, D.R., Doucette, J., Tinetti, M.E., 1994. Predictors

of automobile crashes and moving violations among elderly drivers. Ann. Intern. Med. 121 (11), 842–846.
McGwin Jr., G., Brown, D.B., 1999. Characteristics of traffic crashes among young, middle-aged, and older drivers. Accid. Anal. Prev. 31 (3), 181–198.
Montella, A., 2010. A comparative analysis of hotspot identification methods. Accid. Anal. Prev. 42 (2), 571–581.
Riegl, 2015. Riegl vmx-450 data sheet. RIEGL Laser Measurment Systems.
Road Safety Canada Consulting, 2011. Road Safety in Canada. march 2011 ed.. .
Sarhan, M., Hassan, Y., 2008. Three-dimensional, probabilistic highway design: sight distance application. Transp. Res. Rec. J. Transp. Res. Board 2060, 10–18.
Steel, P., Mesher, D., Adamson, J., 2014. Development of a road safety audit network screening tool. Proceedings of the Twenty-Fourth Canadian Multidisciplinary Road Safety Conference.
Turcotte, M., 2015. Profile of Seniors' Transportation Habits. Statistics Canada.
Wood, J., Donnell, E., 2014. Stopping sight distance and horizontal sight line offsets at horizontal curves. Transp. Res. Rec. J. Transp. Res. Board 2436, 43–50.